Letter

Electromagnetic instability of compact axion stars

Liina M. Chung-Jukko,[1,*] Eugene A. Lim,[1] David J. E. Marsh,[1] Josu C. Aurrekoetxea,[2] Eloy de Jong,[1] and Bo-Xuan Ge[1]

[1]*Physics Department, Theoretical Particle Physics and Cosmology Group, King's College London, Strand, London WC2R 2LS, United Kingdom*

[2]*Astrophysics, University of Oxford, DWB, Keble Road, Oxford OX1 3RH, United Kingdom*

(Received 13 March 2023; accepted 22 August 2023; published 19 September 2023)

If the dark matter is composed of axions, then axion stars are expected to be abundant in the Universe. We demonstrate in fully nonlinear $(3+1)$ numerical relativity the instability of compact axion stars due to the electromagnetic Chern-Simons term. We show that above the critical coupling constant $g_{a\gamma}^{\rm crit} \propto M_s^{-1.35}$, compact axion stars of mass M_s are unstable. The instability is caused by parametric resonance between the axion and the electromagnetic field. The existence of stable compact axion stars requires approximately Planck-suppressed couplings to photons. If the coupling exceeds the critical value, then all stable axion stars are necessarily noncompact. Unstable axion stars decay leaving behind a less massive, less compact, remnant. The emitted radiation peaks at a frequency $\omega \sim 1/R_s$, where R_s is the axion star radius.

DOI: 10.1103/PhysRevD.108.L061302

I. INTRODUCTION

If dark matter (DM) is composed of the QCD axion [1–11] or axionlike particles [12–17] (henceforth, axions), then DM halos are predicted to host an abundance of so-called *axion stars* (see, e.g., Refs. [18–22] for initial formation mechanism, and Ref. [23] for the abundance and merger rates). Axion stars are self-gravitating, time periodic, finite mass solutions of the Klein-Gordon-Einstein equations, which fall under the class of solitonic objects known as oscillatons [24,25].

A defining property of axions is that they are real pseudoscalars, and necessarily couple to gauge fields via the Chern-Simons term. In the case of electromagnetism, this leads to a coupling between the axion and two photons specified by a coupling constant $g_{a\gamma}$ with mass dimension -1. In terms of classical fields, the axion couples to $\vec{E}\cdot\vec{B}$.

It is known that this coupling can lead to an instability of the axion field [26–28]. In particular, within the context of axion stars, this nonlinearity is destabilizing, as was demonstrated in the weak field perturbative regime in Refs. [29,30], and first suggested in Ref. [31]. In the strong field regime, it was also recently shown that complex scalar boson stars with a coupling to the Chern-Simons term can also become unstable [32].

*liina.jukko@kcl.ac.uk

In this paper, we investigate for the first time, the stability of *compact, relativistic* axion stars in the presence of a weak propagating electromagnetic (EM) wave modeling a bath of ambient photons. Objects for which the radius approaches the Schwarszchild radius, $R = 2GM$, are known as *compact* objects where strong gravity effects are of relevance. We therefore use the $3+1$ numerical relativity code GRCHOMBO [33–35] for our results, including strong-field gravitational effects and backreactions. Compact axion stars have $M_s \sim m_{\rm Pl}^2/m$, which is obtained by setting the axion Compton wavelength to the Schwarzschild radius. We use these units to measure axion star mass in our simulations.

We find that, as long as (i) the EM wavelength is approximately the size of the axion star and (ii) the coupling exceeds a critical coupling $g_{a\gamma}^{\rm crit} \propto M_s^{-1.35}$, where M_s is the axion star mass for fixed axion mass m, the star will experience an instability, losing mass via potentially detectable EM emissions.

To be specific, we find the following:

(i) The instability is induced by *parametric resonance*, with an instability band roughly with a bandwidth $\Delta\omega \sim R_s^{-1}$, where R_s is the size of the axion star, centered around $\omega \sim R_s^{-1}$. EM energy is generated exponentially.

(ii) The critical threshold for the coupling is

$$g_{a\gamma}^{\rm crit} \approx \frac{1.66\times10^{-17}}{\rm GeV}\left[\left(\frac{M_s}{M_\odot}\right)\left(\frac{m}{10^{-11}\ {\rm eV}}\right)\right]^{-1.35},$$

where we have chosen to scale our results to $m = 10^{-11}$ eV corresponding to $\mathcal{O}(M_\odot)$ compact axion

stars [36]. We emphasize this result is true for all axion masses m by rescaling symmetry.

(iii) The timescale of the instability is a power law,

$$\tau \propto (g_{a\gamma} - g_{a\gamma}^{\rm crit})^{-0.87},$$

and independent of the initial EM seed amplitude.

(iv) The instability is largely insensitive to the initial amplitude of the ambient EM field E_0—since the instability is exponential, the time to trigger it depends on $t_0 \sim \ln E_0$ at best.

The presence of this instability forbids axion stars from existing above the critical line $g_{a\gamma}^{\rm crit}(M_s)$ in the $(M_s, g_{a\gamma})$ plane, as shown in Fig. 1. Our results imply that stable compact axion stars can exist only if the axion-photon coupling is approximately Planck suppressed. (This instability is in addition to that due to the self-interaction potential [37–40]. Suppressed self-couplings relative to EM couplings are required for the EM instability to dominate; this does not occur for the QCD axion but can in alternative models [41–43].)

II. THEORY

The electromagnetic field strength tensor and its dual are

$$F_{\mu\nu} = \partial_\mu A_\nu - \partial_\nu A_\mu, \qquad \tilde{F}^{\mu\nu} = \frac{1}{2\sqrt{-g}}\varepsilon^{\mu\nu\rho\sigma}F_{\rho\sigma}, \quad (1)$$

with $\varepsilon^{\mu\nu\rho\sigma}$ being the totally antisymmetric Levi-Civita symbol with $\varepsilon^{0123} = +1$. We write the total action as

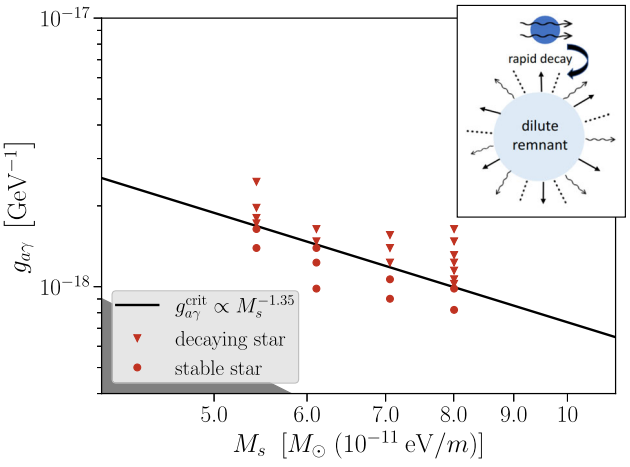

FIG. 1. The critical coupling (in black) along our simulation data (in red), with triangular simulation points representing a decaying star through scalar, electromagnetic, and gravitational radiation (see diagram in top right corner). Our simulations cover $M_s = 0.60, 0.53, 0.46, 0.41 m_{\rm Pl}^2/m$, and we have plotted the mass ranges scaled to $m = 10^{-11}$ eV, which correspond to compact axion stars of $\mathcal{O}(M_\odot)$. Note that our result is true for all axion masses m, which simply rescales the x-axis units.

$$S = \int d^4x\sqrt{-g}\left[\frac{m_{\rm Pl}^2}{16\pi}R - \frac{1}{2}\partial_\mu\phi\partial^\mu\phi - \frac{1}{2}m^2\phi^2 - \frac{1}{4}F_{\mu\nu}F^{\mu\nu} - \frac{g_{a\gamma}}{4}\phi F_{\mu\nu}\tilde{F}^{\mu\nu}\right], \quad (2)$$

where ϕ is the axion field, and R is the Ricci scalar. The last term in this action is the Chern-Simons term, which acts as a boundary term and hence, does not contribute to the stress-tensor. The stress-energy tensor is derived from Eq. (2) to find Einstein's equations $G_{\mu\nu} = 8\pi m_{\rm Pl}^{-2}T_{\mu\nu}$ (see, e.g., Ref. [44]).

The equations of motion in the matter sector are

$$\nabla^\mu\nabla_\mu\phi - m^2\phi = \frac{g_{a\gamma}}{4}F_{\mu\nu}\tilde{F}^{\mu\nu}, \quad (3)$$

$$\nabla_\mu F^{\mu\nu} = -g_{a\gamma}J^\nu, \quad (4)$$

where the current J^ν is defined as $J^\nu = \partial_\mu\phi\tilde{F}^{\mu\nu}$. The parametric resonance is driven by the EM sector Eq. (4), as long as the photon frequency is within the resonance band of the axion field. Since the axion oscillates $\omega \sim m \sim R_s^{-1}$, if the photon wavelength is $\mathcal{O}(R_s)$, resonance will commence.

We solve the full system with numerical relativity using GRCHOMBO [33–35] following the methodology in Refs. [45–49]. For a summary, please see Appendix A. We construct initial conditions for compact axion stars with ADM [50] masses $0.41 m_{\rm Pl}^2/m \le M_s \le 0.60 m_{\rm Pl}^2/m$, which corresponds to

$$5.4M_\odot\left(\frac{10^{-11}\ \text{eV}}{m}\right) \le M_s \le 8.1M_\odot\left(\frac{10^{-11}\ \text{eV}}{m}\right), \quad (5)$$

following the method used in Refs. [24,36,37,40,51–53]. These masses are near the Kaup [54] limit for black hole formation, above which all axion stars are unstable independent of $g_{a\gamma}$.

For the EM field initial conditions, we approximate the initial spacetime as Minkowski, since we are interested in the case where the EM field is subdominant to the energy density of the axion star. This approximation decouples the oscillaton and EM initial conditions from each other, with minimal violations to the initial constraint equations. We choose the components of our gauge field, $A_\mu = C_\mu e^{i(-k_\mu z + \omega_\mu t)}$, to describe a single plane wave polarized in the x direction, with wave vector $k_\mu^{(x)} = (\omega^{(x)}, 0, 0, -k^{(x)})$ such that $\omega^{(x)} = k^{(x)}$ initially. We identify A_0 and A_z with the gauge mode, and set $C_0 = C_z = C_y = 0$ at the initial time. This ansatz satisfies both the Lorenz gauge $k_\mu A^\mu = 0$, and the Bianchi identities, which set the dispersion relation for each wave mode. Using these simplifications, the only nonzero components of the electric and magnetic fields are

$E_x = B_y = -\omega^{(x)} C_x \sin(k^{(x)} z + \omega^{(x)} t)$, where we have used the real part of the gauge fields. We use $k^{(x)} \equiv 2\pi/\lambda \sim 0.10m$, and the amplitude $C_x = 0.001 m_{\rm Pl}$ as our initial conditions. Numerically solving the full nonlinear equations to evolve our system implies that all classical backreactions are included in our simulations. Periodic boundary conditions were used throughout the simulations. We show that the constraint equations are satisfied and tested their convergence during evolution in Appendix B.

III. RESULTS

Slices through our simulation box for the $M_s = 0.60 m_{\rm Pl}^2/m$, and $g_{a\gamma} = 16 m_{\rm Pl}^{-1}$ case illustrating the evolution of the axion and EM energy density are shown in Fig. 2. An incoming seed EM wave (not visible on the scale shown) causes the axion star to emit a strong burst of EM radiation at $t \sim 100 m^{-1}$. At a later time, $t \sim 200 m^{-1}$, the EM radiation becomes less intense, and the axion star begins to settle into a stable lower mass, less compact, and larger configuration. As the star dilutes and increases in radius R_s, its characteristic frequency drifts out of the instability band, shutting down the parametric resonance process.

We next show in Fig. 3 (top panel) the time evolution of the total energy in axions and EM radiation, which can be obtained by integrating their respective energy densities (see Appendix A). In order to describe the decay process, we fit a tanh function for the amplification of the energy of the EM field E_γ,

$$E_\gamma(t) = A\left(\frac{e^{2(t-t_0)/\tau}+1}{e^{2(t-t_0)/\tau}-1}\right) + B, \tag{6}$$

where the constants A and B depend on the simulation box size.

The amplification in the EM energy sets two timescales: the parameter t_0 determines how fast the amplification process begins after the start of the simulation, and τ can be seen as a measure of the lifetime of the star in the decay process. The dependence of t_0 and τ on the axion-photon coupling $g_{a\gamma}$ is demonstrated in Fig. 3 (bottom panel); they follow a decaying power law, which has an asymptote at a critical value of $g_{a\gamma} \approx 12.1 m_{\rm Pl}^{-1}$ based on our simulation data. We find $\tau \propto g_{a\gamma}^{-0.87}$. We compare this result to the parametric resonance instability timescale for a homogeneous cosmological axion field, which is proportional to $g_{a\gamma}^{-1}$, although the instability is blocked by the expansion of the Universe [8]. A gravitational potential well, provided by the axion star itself, is required to allow for the

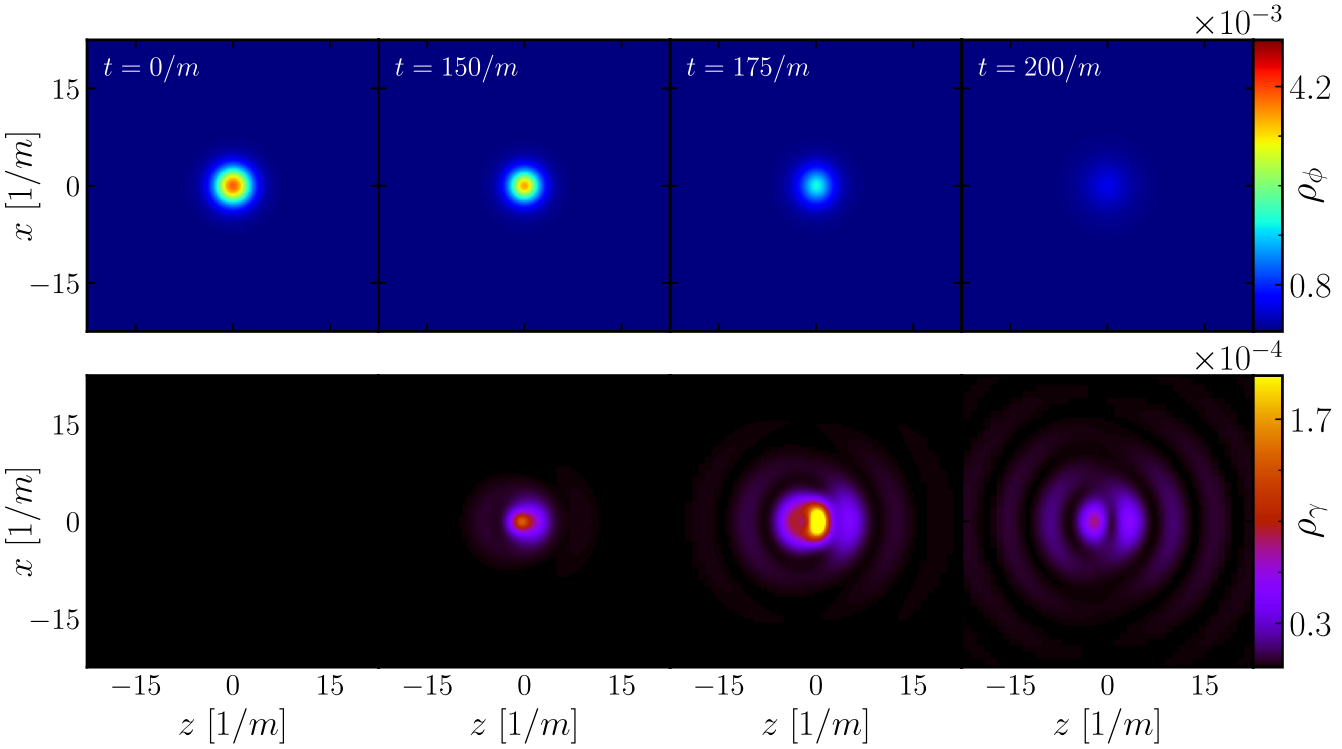

FIG. 2. Energy densities of the electromagnetic and scalar fields as a slice through the centre of the star for the $M_s = 0.60 m_{\rm Pl}^2/m$, $g_{a\gamma} = 16 m_{\rm Pl}^{-1}$ case. The EM field (bottom panel), initially polarized in the x direction, is initially propagating from the right to the left. As parametric resonance kicks in, the axion star undergoes rapid dilution and mass loss, with a corresponding burst in the EM energy which is roughly isotropic (see $t = 175/m$). The process stops when the axion star dilutes and expands to a size away from the characteristic frequency of the EM spectra. A movie of our simulations for coupling $g_{a\gamma} = 16 m_{\rm Pl}^{-1}$ can be found in [55].

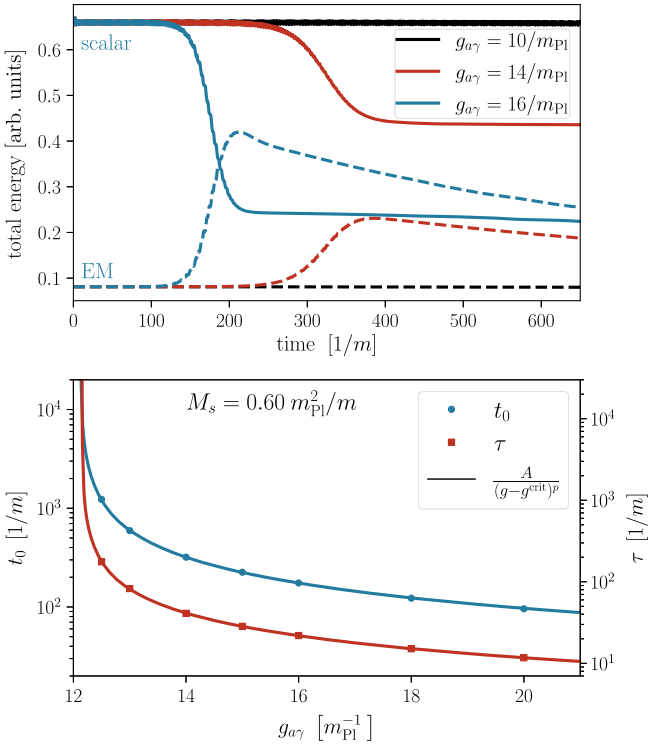

FIG. 3. *Top:* The total energy in the scalar (solid line) and electromagnetic fields (dashed line) for several values of the coupling $g_{a\gamma}$ for the $M_s = 0.60 m_{\rm Pl}^2/m$ case. Total energy conservation (including gravitational energy) is checked by ensuring the Hamiltonian constraint is not violated (see Appendix B). *Bottom:* The values of the parameters t_0 and τ from the hyperbolic tangent fit Eq. (6) to the EM energy profile as a function of the axion-photon coupling $g_{a\gamma}$. The power law function fitted can be seen in the legend. This gives a critical value for the coupling of $\sim 12.1 m_{\rm Pl}^{-1}$. The simulation errors found through higher resolution runs were of order 0.1% for t_0 and 1% for τ. The values for $g^{\rm crit}$ and p were $12.1 m_{\rm Pl}^{-1}$ and 0.83, respectively, for t_0, and $12.2 m_{\rm Pl}^{-1}$ and 0.87 for τ.

instability to develop [31]. Our results indicate that the decay scaling for relativistic highly inhomogeneous compact axion stars is comparable but different from the homogeneous case.

We verified the dependence of t_0 and τ on the EM seed amplitude. We find that τ is independent of the amplitude for fixed photon-axion coupling $g_{a\gamma}$. We note that A from Eq. (6) is also constant, indicating that the EM field is amplified by the same amount of energy, and hence, the amplification has the same shape independent of the amplitude of the EM seed E_0. Furthermore, we confirm that t_0 has a logarithmic dependence on the initial amplitude of the EM seed, $t_0 \sim \ln E_0$ [e.g., we find $t_0 \approx -31.3 m^{-1} \ln(1860 (m_{\rm Pl} m)^{-1} E_0) + 174 m^{-1}$ for $M_s = 0.60 m_{\rm Pl}^2/m$ and $g_{a\gamma} = 15 m_{\rm Pl}^{-1}$, with the constants being parameter dependent], as the growth of the EM field is an exponential process $E(t) \sim E_0 \exp((t - t_0)/\tau)$.

Weak field calculations of nonrelativistic (and hence, noncompact) axion star decay suggest a critical value for the axion-photon coupling $g_{a\gamma}^{\rm crit} = 7.66 m_{\rm Pl}/\sqrt{8\pi m M_s}$, or $g_{a\gamma}^{\rm crit} \propto M_s^{-1}$ [30]. While the power law is different, the proximity of the coefficient suggests that decay dynamics are broadly similar in both the weak and strong gravity limits (in agreement with complex scalar boson stars [32]). A possible explanation is that it is driven by *matter* couplings, with gravity playing only a second order role (see, e.g., Refs. [56,57]). We also compared the critical mass given in Ref. [30] to the remnant axion star mass from our simulations and find they were of the same order of magnitude with our remnants having slightly lower mass.

In Fig. 4, we show the power spectra $P(k)$ of the x, y, and z components of the electric field at $t = 350 m^{-1}$ for $g_{a\gamma} = 16 m_{\rm Pl}^{-1}$, after the decay process has happened, along with the original seed (black dashed line), demonstrating the frequency of the EM radiation emitted by the axion star as it decays. We obtained the power spectrum by performing a fast Fourier transform on the spatial electric field and then integrating the square of the transform in k space. We note two salient points. First, around the incoming frequency $k = 0.1m$, the E_x power broadens, with a corresponding smaller power in E_z and E_y power, but no large amplification. Second, the primary power of the emission lies around $k \sim 0.5m$, equipartitioned between the x, y and z components. This scale corresponds to the diameter $2R_s$ of the axion star $2kR_s \sim 2\pi$, $k \sim 0.6m$, capturing the emission from parametric resonance. This equipartition of energies arises from (i) the total momentum of the system must remain small as the initial EM waves carry negligible

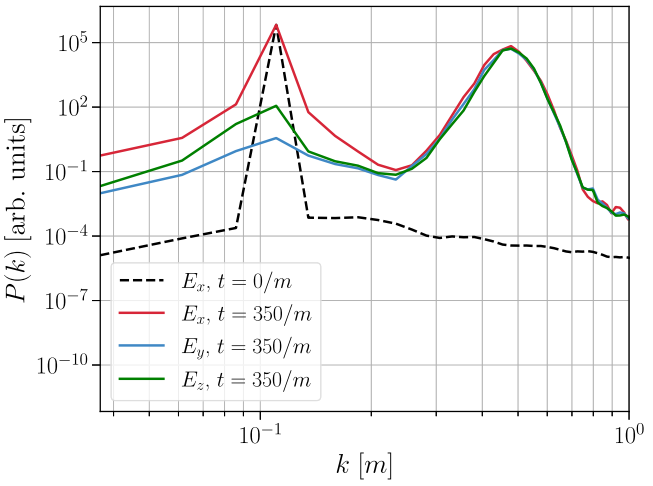

FIG. 4. Power spectra of the electric field for $g_{a\gamma} = 16 m_{\rm Pl}^{-1}$ at time $t = 350 m^{-1}$, which is after the decay process has ended, for the $M_s = 0.60 m_{\rm Pl}^2/m$. The excitation of the wave mode corresponding to the inherent frequency scale of the axion star around $k \sim 0.5m$ is clearly visible, where the energy is equipartitioned. The black dashed line demonstrates the power spectrum of the initial EM seed, polarized in the x direction.

momenta, and (ii) the source current for the radiation is the initially spherically symmetric axion star $J_\mu \propto \partial_\mu \phi$. We note that while we saw evidence of birefringence between the x and y components before decay, postdecay this effect is subdominant. We leave to future work a complete study of the emission power and possibly circularly polarized emission due to CP violation.

IV. CONCLUSIONS

We have demonstrated in fully nonlinear simulations that axion stars are unstable above a critical line $g_{a\gamma}^{\rm crit} \propto M_s^{-1.35}$ in the plane of mass and coupling constant, exploding into EM radiation. Crucially, we have shown this decay process with a log dependence on the amplitude of the plane wave, suggesting that ambient radiation alone would be sufficient to destabilize compact axion stars on Hubble timescales. As an example, assuming the resonant band $\delta\omega \sim m$ and $g_{a\gamma} = 15 m_{\rm Pl}^{-1}$, destabilization of $\mathcal{O}(M_\odot)$ compact axion stars stimulated by the cosmic microwave background photons will take approximately $t_0 \sim 0.05$ seconds, smaller than the Hubble expansion time by many orders of magnitude.

If axion stars are unstable above a critical mass, one might ask how such unstable stars might form in the first place, and what the observable consequences are. In hierarchical structure formation, the lightest axion stars form first in low mass dark matter halos near the axion Jeans scale [18]. These lightest axion stars will be stable and can grow to criticality via (major) mergers. We have shown in two related works to this one [23,58] how the axion star formation and merger rate can be computed, and how the resulting radio emission leads to a new channel for indirect axion detection via heating of the intergalactic medium. High compactness axion stars, like the ones studied in this work, are required for their mergers to produce observable gravitational waves [59], with axion masses $m \sim 10^{-11}$ eV placing the high compactness stars in the LIGO frequency band (hence, our reference mass choices throughout this work). The required high compactness seeds can be formed by direct collapse of primordial perturbations [20] or under modified thermal histories [60].

ACKNOWLEDGMENTS

We would like to thank Thomas Helfer for his early contribution to the project. We also thank members of the GRCHOMBO Collaboration for technical support and help. L. M. C. J. is supported by a studentship funded by the Science and Technologies Facilities Council (U.K.). D. J. E. M. is supported by an Ernest Rutherford Fellowship from the Science and Technologies Facilities Council (No. ST/T004037/1). J. C. A. acknowledges funding from the Beecroft Trust and The Queen's College via an extraordinary Junior Research Fellowship (eJRF). This work used the DiRAC@Durham Cosma facility managed by the Institute for Computational Cosmology on behalf of the STFC DiRAC HPC Facility (www.dirac.ac.uk), under DiRAC Grant No. ACTP238. The equipment was funded by BEIS capital funding via STFC Capital Grants No. ST/P002293/1, No. ST/R002371/1, and No. ST/S002502/1, Durham University and STFC Operations Grant No. ST/R000832/1.

APPENDIX A: NUMERICAL METHODOLOGY

Our numerical implementation on GRCHOMBO [33–35] evolves the gravity sector using the CCZ4 formalism [61,62], together with the integrated moving puncture gauge [63,64]. The decomposition of the matter sector is based on [46] (see Appendix A in that paper in particular), with an additional Chern-Simons coupling between the EM and scalar sector,

$$L_{\rm CS} = -\frac{g_{a\gamma}}{4}\phi F_{\mu\nu}\tilde{F}^{\mu\nu},$$

and no gauge coupling (i.e., $e = 0$).

We use as diagnostic quantities the energy densities in both the scalar $\rho_\phi = n^\mu n^\nu T^\phi_{\mu\nu}$ and the EM field $\rho_\gamma = n^\mu n^\nu T^\gamma_{\mu\nu}$, which are obtained projecting their respective energy momentum tensor with the normal vector n^μ to the three-dimensional hypersurface. In terms of the fields, these are expressed as

$$T^\phi_{\mu\nu} = \nabla_\mu\phi\nabla_\nu\phi - \frac{g_{\mu\nu}}{2}(\nabla_\sigma\phi\nabla^\sigma\phi + m^2\phi^2), \quad \text{(A1)}$$

$$T^\gamma_{\mu\nu} = F_{\mu\alpha}F^\alpha{}_\nu - \frac{1}{4}g_{\mu\nu}F_{\alpha\beta}F^{\alpha\beta}. \quad \text{(A2)}$$

Note that the Chern-Simons term does not contribute to the stress tensor as it is topological. The total energy in axions and the EM field can then be calculated integrating the energy densities over a volume V,

$$E_{\{\phi,\gamma\}} = \int_V \sqrt{\gamma}\rho_{\{\phi,\gamma\}}dV. \quad \text{(A3)}$$

APPENDIX B: CONVERGENCE TESTING

We monitor the evolution of the average Hamiltonian and momentum constraints in a sphere of radius $64m^{-1}$ centered around the axion star. For the initial conditions of the (subdominant) EM field, we approximate the initial spacetime as Minkowski, which introduces minimal violations to the constraints that are quickly damped via CCZ4. In addition, we checked that the gauge field constraint violation was negligible and under control throughout the simulations.

We tested convergence for the $g_{a\gamma} = 16 m_{\rm Pl}^{-1}$ case comparing the evolution of the Hamiltonian and momentum constraint violations for two resolutions in a simulation with box size $L = 256m^{-1}$ and seven refinement levels. For the low and high resolutions, we increased the number

of coarse grid points from $N^3 = 128^3$ to $N^3 = 192^3$, resulting in finest grid sizes of $\Delta x \approx 1.6 \times 10^{-2} m^{-1}$ and $\Delta x \approx 10^{-2} m^{-1}$, respectively.[1] In Fig. 5, we show how the errors in the Hamiltonian and momentum constraints were reduced by a factor consistent with second order convergence when the resolution was increased.

One might worry about the self-amplification of the EM field due to the periodic boundary conditions. By doubling the size of the simulation box, we tested that the evolution of the EM field was not altered by the reflected energy density until the resonance phase had finished (but can spoil the second order convergence of the constraints as shown in Fig. 5).

Additionally, we found that the postdecay electromagnetic energy density in Fig. 3 drops due to the fact that the standard resolution used in our simulations cannot track the highest frequency modes generated during the resonant phase. The Kreiss-Oliger dissipation used in GRCHOMBO to remove the noise introduced by regridding also removes EM modes with wavelengths of the order of the grid spacing. We checked that these higher modes can be recovered by increasing the resolution of the simulation, and estimated that the errors in the physical variables characterizing the amplification of the EM field (see Fig. 3) are negligible—order 1% at most. For the case of nondecaying stars, we evolved the system until $t \approx 1500/m$.

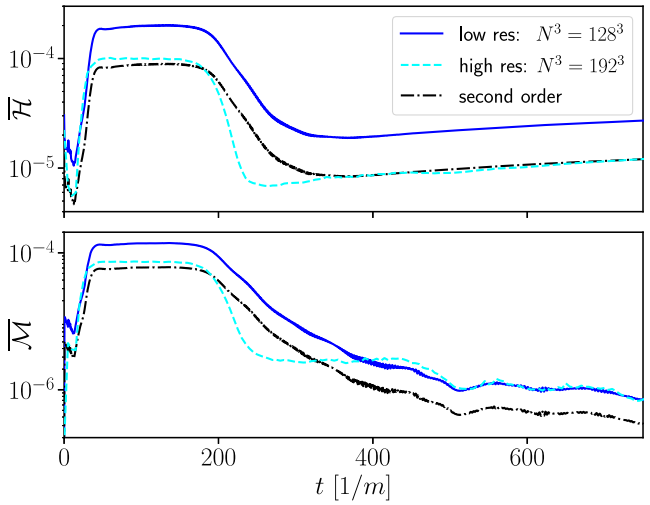

FIG. 5. Convergence test of the average Hamiltonian $\bar{\mathcal{H}}$ and momentum constraint $\bar{\mathcal{M}}$ violations in a sphere of radius $64m^{-1}$ centered around the axion star. Simulation box size is $L = 256m^{-1}$, and low and high resolution runs have $N^3 = 128^3$ and $N^3 = 192^3$ number of coarse grid points, respectively.

[1]Note that the size of the axion star is $R_s \sim m^{-1}$, implying that it is resolved with $\mathcal{O}(100)$ number of grid points.

[1] R. D. Peccei and H. R. Quinn, *CP* Conservation in the Presence of Instantons, Phys. Rev. Lett. **38**, 1440 (1977).
[2] S. Weinberg, A New Light Boson?, Phys. Rev. Lett. **40**, 223 (1978).
[3] F. Wilczek, Problem of Strong p and t Invariance in the Presence of Instantons, Phys. Rev. Lett. **40**, 279 (1978).
[4] J. E. Kim, Weak Interaction Singlet and Strong *CP* Invariance, Phys. Rev. Lett. **43**, 103 (1979).
[5] M. A. Shifman, A. I. Vainshtein, and V. I. Zakharov, Can confinement ensure natural *CP* invariance of strong interactions?, Nucl. Phys. **B166**, 493 (1980).
[6] M. Dine, W. Fischler, and M. Srednicki, A simple solution to the strong *CP* problem with a harmless axion, Phys. Lett. **104B**, 199 (1981).
[7] A. R. Zhitnitsky, On possible suppression of the axion hadron interactions. (In Russian), Sov. J. Nucl. Phys. **31**, 260 (1980).
[8] J. Preskill, M. B. Wise, and F. Wilczek, Cosmology of the invisible axion, Phys. Lett. **120B**, 127 (1983).
[9] L. F. Abbott and P. Sikivie, A cosmological bound on the invisible axion, Phys. Lett. **120B**, 133 (1983).
[10] M. Dine and W. Fischler, The not so harmless axion, Phys. Lett. **120B**, 137 (1983).
[11] L. Di Luzio, M. Giannotti, E. Nardi, and L. Visinelli, The landscape of QCD axion models, Phys. Rep. **870**, 1 (2020).
[12] M. S. Turner, Coherent scalar field oscillations in an expanding universe, Phys. Rev. D **28**, 1243 (1983).
[13] E. Witten, Some properties of O(32) superstrings, Phys. Lett. **149B**, 351 (1984).
[14] M. Khlopov, B. A. Malomed, and I. B. Zeldovich, Gravitational instability of scalar fields and formation of primordial black holes, Mon. Not. R. Astron. Soc. **215**, 575 (1985).
[15] P. Svrcek and E. Witten, Axions in string theory, J. High Energy Phys. 06 (2006) 051.
[16] P. Arias, D. Cadamuro, M. Goodsell, J. Jaeckel, J. Redondo, and A. Ringwald, WISPy cold dark matter, J. Cosmol. Astropart. Phys. 06 (2012) 013.
[17] D. J. E. Marsh, Axion cosmology, Phys. Rep. **643**, 1 (2016).
[18] H.-Y. Schive, T. Chiueh, and T. Broadhurst, Cosmic structure as the quantum interference of a coherent dark wave, Nat. Phys. **10**, 496 (2014).
[19] D. G. Levkov, A. G. Panin, and I. I. Tkachev, Gravitational Bose-Einstein Condensation in the Kinetic Regime, Phys. Rev. Lett. **121**, 151301 (2018).

[20] J. Y. Widdicombe, T. Helfer, D. J. E. Marsh, and E. A. Lim, Formation of relativistic axion stars, J. Cosmol. Astropart. Phys. 10 (2018) 005.
[21] B. Eggemeier and J. C. Niemeyer, Formation and mass growth of axion stars in axion miniclusters, Phys. Rev. D **100**, 063528 (2019).
[22] J. Chen, X. Du, E. W. Lentz, D. J. E. Marsh, and J. C. Niemeyer, New insights into the formation and growth of boson stars in dark matter halos, Phys. Rev. D **104**, 083022 (2021).
[23] X. Du, D. J. E. Marsh, M. Escudero, A. Benson, D. Blas, C. K. Pooni, and M. Fairbairn, Soliton merger rates and enhanced axion dark matter decay, arXiv:2301.09769.
[24] E. Seidel and W. M. Suen, Oscillating Soliton Stars, Phys. Rev. Lett. **66**, 1659 (1991).
[25] E. Seidel and W.-M. Suen, Formation of Solitonic Stars through Gravitational Cooling, Phys. Rev. Lett. **72**, 2516 (1994).
[26] T. W. Kephart and T. J. Weiler, Luminous axion clusters, Phys. Rev. Lett. **58**, 171 (1987).
[27] M. Boskovic, R. Brito, V. Cardoso, T. Ikeda, and H. Witek, Axionic instabilities and new black hole solutions, Phys. Rev. D **99**, 035006 (2019).
[28] T. Ikeda, R. Brito, and V. Cardoso, Blasts of Light from Axions, Phys. Rev. Lett. **122**, 081101 (2019).
[29] M. P. Hertzberg and E. D. Schiappacasse, Dark matter axion clump resonance of photons, J. Cosmol. Astropart. Phys. 11 (2018) 004.
[30] D. G. Levkov, A. G. Panin, and I. I. Tkachev, Radio-emission of axion stars, Phys. Rev. D **102**, 023501 (2020).
[31] I. I. Tkachev, An axionic laser in the center of a galaxy?, Phys. Lett. B **191**, 41 (1987).
[32] N. Sanchis-Gual, M. Zilhão, and V. Cardoso, Electromagnetic emission from axionic boson star collisions, Phys. Rev. D **106**, 064034 (2022).
[33] K. Clough, P. Figueras, H. Finkel, M. Kunesch, E. A. Lim, and S. Tunyasuvunakool, GRChombo: Numerical relativity with adaptive mesh refinement, Classical Quantum Gravity **32**, 245011 (2015).
[34] T. Andrade *et al.*, GRChombo: An adaptable numerical relativity code for fundamental physics, J. Open Source Software **6**, 3703 (2021).
[35] M. Radia, U. Sperhake, A. Drew, K. Clough, P. Figueras, E. A. Lim, J. L. Ripley, J. C. Aurrekoetxea, T. França, and T. Helfer, Lessons for adaptive mesh refinement in numerical relativity, Classical Quantum Gravity **39**, 135006 (2022).
[36] M. Alcubierre, R. Becerril, S. F. Guzman, T. Matos, D. Nunez, and L. A. Urena-Lopez, Numerical studies of Phi**2 oscillatons, Classical Quantum Gravity **20**, 2883 (2003).
[37] T. Helfer, D. J. E. Marsh, K. Clough, M. Fairbairn, E. A. Lim, and R. Becerril, Black hole formation from axion stars, J. Cosmol. Astropart. Phys. 03 (2016) 055.
[38] D. G. Levkov, A. G. Panin, and I. I. Tkachev, Relativistic Axions from Collapsing Bose Stars, Phys. Rev. Lett. **118**, 011301 (2017).
[39] L. Visinelli, S. Baum, J. Redondo, K. Freese, and F. Wilczek, Dilute and dense axion stars, Phys. Lett. B **777**, 64 (2018).
[40] F. Michel and I. G. Moss, Relativistic collapse of axion stars, Phys. Lett. B **785**, 9 (2018).
[41] K. Choi, S. H. Im, and C. Sub Shin, Recent progress in the physics of axions and axion-like particles, Annu. Rev. Nucl. Part. Sci. **71**, 225 (2021).
[42] M. Farina, D. Pappadopulo, F. Rompineve, and A. Tesi, The photo-philic QCD axion, J. High Energy Phys. 01 (2016) 095.
[43] A. V. Sokolov and A. Ringwald, Electromagnetic couplings of axions, arXiv:2205.02605.
[44] E. V. Gorbar, K. Schmitz, O. O. Sobol, and S. I. Vilchinskii, Gauge-field production during axion inflation in the gradient expansion formalism, Phys. Rev. D **104**, 123504 (2021).
[45] M. Zilhão, H. Witek, and V. Cardoso, Nonlinear interactions between black holes and Proca fields, Classical Quantum Gravity **32**, 234003 (2015).
[46] T. Helfer, J. C. Aurrekoetxea, and E. A. Lim, Cosmic string loop collapse in full general relativity, Phys. Rev. D **99**, 104028 (2019).
[47] C. Gundlach, J. M. Martin-Garcia, G. Calabrese, and I. Hinder, Constraint damping in the Z4 formulation and harmonic gauge, Classical Quantum Gravity **22**, 3767 (2005).
[48] C. Palenzuela, L. Lehner, and S. Yoshida, Understanding possible electromagnetic counterparts to loud gravitational wave events: Binary black hole effects on electromagnetic fields, Phys. Rev. D **81**, 084007 (2010).
[49] D. Hilditch, An introduction to well-posedness and free-evolution, Int. J. Mod. Phys. A **28**, 1340015 (2013).
[50] R. L. Arnowitt, S. Deser, and C. W. Misner, The dynamics of general relativity, Gen. Relativ. Gravit. **40**, 1997 (2008).
[51] T. Helfer, E. A. Lim, M. A. G. Garcia, and M. A. Amin, Gravitational wave emission from collisions of compact scalar solitons, Phys. Rev. D **99**, 044046 (2019).
[52] L. A. Urena-Lopez, T. Matos, and R. Becerril, Inside oscillatons, Classical Quantum Gravity **19**, 6259 (2002).
[53] L. A. Urena-Lopez, Oscillatons revisited, Classical Quantum Gravity **19**, 2617 (2002).
[54] D. J. Kaup, Klein-Gordon Geon, Phys. Rev. **172**, 1331 (1968).
[55] https://www.youtube.com/watch?v=5UC_PymwAIU.
[56] M. A. Amin and Z.-G. Mou, Electromagnetic bursts from mergers of oscillons in axion-like fields, J. Cosmol. Astropart. Phys. 02 (2020) 024.
[57] M. A. Amin, A. J. Long, and E. D. Schiappacasse, Photons from dark photon solitons via parametric resonance, J. Cosmol. Astropart. Phys. 05 (**2023**) 015.
[58] M. Escudero, C. K. Pooni, M. Fairbairn, D. Blas, X. Du, and D. J. E. Marsh, Axion star explosions: A new source for axion indirect detection, arXiv:2302.10206.
[59] G. F. Giudice, M. McCullough, and A. Urbano, Hunting for dark particles with gravitational waves, J. Cosmol. Astropart. Phys. 10 (2016) 001.
[60] A. L. Erickcek and K. Sigurdson, Reheating effects in the matter power spectrum and implications for substructure, Phys. Rev. D **84**, 083503 (2011).
[61] D. Alic, C. Bona-Casas, C. Bona, L. Rezzolla, and C. Palenzuela, Conformal and covariant formulation of the Z4 system with constraint-violation damping, Phys. Rev. D **85**, 064040 (2012).

[62] D. Alic, W. Kastaun, and L. Rezzolla, Constraint damping of the conformal and covariant formulation of the Z4 system in simulations of binary neutron stars, Phys. Rev. D **88**, 064049 (2013).

[63] M. Campanelli, C. O. Lousto, P. Marronetti, and Y. Zlochower, Accurate Evolutions of Orbiting Black-Hole Binaries without Excision, Phys. Rev. Lett. **96**, 111101 (2006).

[64] J. G. Baker, J. Centrella, D.-I. Choi, M. Koppitz, and J. van Meter, Gravitational Wave Extraction from an Inspiraling Configuration of Merging Black Holes, Phys. Rev. Lett. **96**, 111102 (2006).